Turkish Journal of Engineering

CRITICALITY CALCULATION OF A HOMOGENOUS CYLINDRICAL NUCLEAR REACTOR CORE USING FOUR-GROUP DIFFUSION EQUATIONS

Babatunde Michael Ojo *[1], Musibau Keulere Fasasi [2], Ayodeji Olalekan Salau [3], Stephen Friday Olukotun [4] and Mathew Ademola Jayeola [5]

[1] Obafemi Awolowo University, Science Faculty, Physics and Engineering Physics Department, Ile-Ife, Nigeria
ORCID ID 0000-0002-2217-7654
Ojobabatundemichael@gmail.com

[2] Obafemi Awolowo University, Science Faculty, Center for Energy and Research Development, Ile-Ife, Nigeria
ORCID ID 0000-0002-4056-173X
mfasasi2001@yahoo.com

[3] Obafemi Awolowo University, Technology Faculty, Electronic and Electrical Engineering Department, Ile-Ife, Nigeria
ORCID ID 0000-0002-6264-9783
ayodejisalau98@gmail.com

[4] Obafemi Awolowo University, Science Faculty, Physics and Engineering Physics Department, Ile-Ife, Nigeria
ORCID ID 0000-0002-7409-5466
olukotunsf@gmail.com

[5] Obafemi Awolowo University, Science Faculty, Physics and Engineering Physics Department, Ile-Ife, Nigeria
ORCID ID 0000-0002-3131-3187
senatormao6@gmail.com

* Corresponding Author
Received: 01/04/2018   Accepted: 04/05/2018

ABSTRACT

In this study, we present a general equation for Finite Difference Method Multi-group Diffusion (FDMMD) equations of a cylindrical nuclear reactor core. In addition, we developed an algorithm which we called TUNTOB for solving the FDMMD equations, determined the fluxes at each of the mesh points and calculated the criticality of the four energy group. This was with a view to using the four-group diffusion equations to estimate the criticality of a cylindrical reactor core that will be accurate and locally accessible for nuclear reactor design in developing countries. The multi-group diffusion equations were solved numerically by discretization using the Finite Difference Method (FDM) to obtain a general equation for a cylindrical reactor core. The fluxes at each mesh point and the criticality of the four energy group were then determined. From the results obtained, we observed that an increment in iteration led to an increase in the effective multiplication factor (k_{eff}) with a corresponding increase in the computation time. A maximum effective multiplication factor was reached when the number of iteration was 1000 and above. Having established the optimal number of iterations, the effects of the mesh sizes on the computation examined revealed that the values of k_{eff} increases as the mesh sizes becomes smaller until an optimal mesh size of 1 x 1 cm^2 was reached and further decrease in mesh sizes gave no further improvement in the value of k_{eff}. The Study concluded that the accuracy in the values of k_{eff} and the smoothness of the neutron distribution curves in 3-D representations depend on the number of mesh points.

Keywords: Four-group diffusion equation, Effective multiplication factor, Mesh size, Reactor, Criticality calculation

1. INTRODUCTION

The criticality of a system containing fissionable materials is described by its effective multiplication factor (k_{eff}). The effective multiplication factor is the ratio of the number of neutrons in one generation to the number of neutrons in the previous generation as shown in Eq. (**1**). A generation is essentially the lifetime of a neutron, in a finite system, the effective multiplication factor is denoted as $k_{effective}$ or k_{eff}, which is used to determine the stability of a nuclear reactor core. When a system is critical, it maintains a steady–state chain reaction of nuclear fissioning, and k_{eff} = 1. The average neutron population in a critical system stays constant in time. A sub-critical system has k_{eff} < 1 and the neutron population dies off in time. The neutron population in a super-critical system, where k_{eff} > 1, grows without bound in time (Urbatsch, 1995).

$$k_{eff} = \frac{Number\ of\ neutrons\ in\ one\ generation}{Number\ of\ neutrons\ in\ the\ preceding\ generation}$$ (1)

The knowledge of k_{eff} is necessary when designing nuclear reactors. However, numerical methods are used almost exclusively for criticality calculations (Urbatsch, 1995). Different numerical methods have been proposed to solve the two group neutron diffusion equations with little attention to the other groups. Although, the two group neutron diffusion equations do not give a detailed explanation of neutron flux distribution in a practical nuclear reactor core, the four-group neutron diffusion equations are known to give a far better description of neutron distribution in a practical nuclear reactor core. Hence the study of the criticality of the cylindrical reactor core and its calculation using four-group diffusion equations by applying the finite difference method (FDM).

The remainder of this paper is organized as follows. In Section 2, a review of related works is provided, while a detailed explanation of the discretization of the four group diffusion equations using finite difference method is given in Section 3. In Section 4, the results are presented and discussed and Section 5 concludes this paper.

2. NUCLEAR REACTOR CORE

A nuclear reactor core is a part of a nuclear reactor which contains the nuclear fuel components where all the nuclear reactions takes place and consequently heat is generated from the reaction. In addition, a nuclear reactor produces and controls the release of energy in form of heat from the splitting of the atoms of uranium.

2.1. Neutron-Nucleus Reactions

It is important to recognize that since neutrons are electrically neutral, they are unaffected by the electrons in the atom or by the positive charge of the nucleus. As a consequence, neutrons pass through the atomic electron cloud and interact directly with the nucleus. Neutrons collide with nuclei, not with atoms (Larmash and Baratta, 2001).

The operation of a reactor basically depends on how neutrons interact with nuclei in the reactor. There are various types of known neutron interactions which could be considered as shown in Fig. 1 (Arzhanov, 2010). All neutron reactions can be categorized as either elastic or inelastic collisions, on the condition that either the kinetic energy is conserved in the collision or not. (Burnham, 1967).

2.1.1. Neutron Flux

Neutron flux is defined as the product of the neutron density and the velocity,

$$\phi = nv$$ (2)

so that it is expressed in units of neutrons per cm^2 per second. It is equal to the total distance (sum of all the path lengths) travelled in one second by all the neutrons present in one cm^3.

In a reactor, the values of neutron density and neutron flux are a function of location in the core. Because the neutron flux is an essential ingredient in the computation of reactor rates, the determination of the spatial distribution of the neutron flux in the core is an important part of reactor physics. The value of the neutron flux at a given point in the core will depend on the distribution of nuclear properties like the cross sections throughout the core, and on the position in relation to the central part of the core and to the external surface of the reactor. The neutron flux continually drops to zero at, or just beyond, the radial and axial boundaries of the core. The behavior of the flux in the core and its rate of decline towards the boundaries must be calculated by means of computer codes (AECBC, 1993; Jayeola *et al.*, 2018).

2.1.2. The Neutron Diffusion Equation

The neutron diffusion equations provide an essential exact description of the neutron distribution within a reactor. Its solution would contain essentially all the information we require concerning the nuclear behavior of the reactor (Duderstadt and Hamilton, 1976).

The multi-group diffusion equation comprises of the groups of neutrons of different energies diffusing within a nuclear reactor. The basic diffusion equation for each group of neutrons is the same, but with absorption generalized to all processes that remove the neutron from the group that is absorption plus scattering to another group and with the source of neutrons for each group specialized to include the in-scattering of neutrons from the other groups, which is also diffusing within the reactor (Stacey, 2007).

2.1.3. Numerical Methods used in neutron diffusion equation

It is assumed that a uniform reactor has the shape of a cylinder of physical radius (R) and height (H). This finite cylindrical reactor has cylindrical geometry which have coordinates at its origin. In order to solve the diffusion equations, the Laplacian is replaced by its

cylindrical form: cylindrical coordinates - 3D, 2D. This is not dependent on angle Θ, therefore, the 3D Laplacian is replaced by its two-dimensional form (2D). This makes it practicable to solve the problem using radial and axial directions. This is because the flux is a function of radius – r and height – z only (Φ(r, z)).

Furthermore, numerical solutions of neutron diffusion equations have been solved using a number of numerical methods such as the finite difference, finite element, nodal and boundary element methods. These methods are all mesh-based in which the nodes that discretize the problem domain are related in a predefined manner (Tanbay and Bilge, 2013). However, numerical methods are used most exclusively for criticality calculations. Criticality calculations k_{eff} are based on power iteration procedures, where different multi-group diffusion equations with a number of iterations are used to estimate the effective multiplication factor (k_{eff}). This iteration process is repeated until the fission distribution has converged.

3. METHODOLOY

3.1. Calculation of the Four-Group Diffusion Equations

To calculate the four-group diffusion equation, we use the finite difference discretization of steady state four-group neutron diffusion equation in a cylindrical coordinate. First, the finite difference discretization of one group differential equation was established and later extended to four-group differential equation. The boundary conditions introduced in this research are: the neutron flux vanishes at the extrapolated boundary of the core (r = R and z = 0, H). Where R = Extrapolated Radius and H = Extrapolated Height. The multi-group diffusion system in a cylindrical coordinate can be written as:

$$\frac{1}{r}\frac{\partial}{\partial r}\left[D(r,z)r\frac{\partial\varphi(r,z)}{\partial r}\right] + \frac{\partial}{\partial z}\left[D(r,z)\frac{\partial\varphi(r,z)}{\partial z}\right]$$

$$-\sum_t(r,z)\varphi(r,z)$$

$$= -S(r,z) \tag{3}$$

The dependent variable in Eq. (3) is the neutron flux, D is the diffusion coefficient and S is the neutron fission source used to initiate the fission reaction. The third term in Eq. (3), (sigma subscript 't') is the total macroscopic cross section of the reactor core.

Multiplying Eq. (3) through by r, we obtain:

$$\frac{\partial}{\partial r}\left[D(r,z)r\frac{\partial\varphi(r,z)}{\partial r}\right] + \frac{\partial}{\partial z}\left[rD(r,z)\frac{\partial\varphi(r,z)}{\partial z}\right] - r\sum_t(r,z)\varphi(r,z) = -rS(r,z) \tag{4}$$

The Eq. (4) was discretized using a finite difference method to obtain the four-group diffusion equations by considering the neutron flux varying along the radial and axial coordinate, hence the Fick's law for the radial and axial coordinate can be written as Eqs. (5) and (6) respectively:

$$J = D(r,z)r\frac{\partial\varphi(r,z)}{\partial r} \tag{5}$$

and

$$Y = D(r,z)\frac{\partial\varphi(r,z)}{\partial z} \tag{6}$$

where J and Y are the neutron current density for the radial and axial coordinates respectively.
Substituting Eq. (5) and Eq. (6) into Eq. (4), we obtain Eq. (7).

$$\frac{\partial J}{\partial r} + r\frac{\partial Y}{\partial z} - r\,\Sigma_t(r,z)\varphi(r,z) = -rS(r,z) \tag{7}$$

The reactor is assumed to cover a special mesh of r and z dimensions as shown in the Fig. 2. Hence Eq. (7) is solved by integrating over the mesh intervals, to obtain:

$$\int_{r_{i-1/2}}^{r_{i+1/2}}\int_{z_{j-1/2}}^{z_{j+1/2}}\frac{\partial J}{\partial r}drdz + r\int_{r_{i-1/2}}^{r_{i+1/2}}\int_{z_{j-1/2}}^{z_{j+1/2}}\frac{\partial Y}{\partial r}drdz - r\int_{r_{i-1/2}}^{r_{i+1/2}}\int_{z_{j-1/2}}^{z_{j+1/2}}\Sigma_t\varphi(r,z)drdz = \int_{r_{i-1/2}}^{r_{i+1/2}}\int_{z_{j-1/2}}^{z_{j+1/2}}rSgdrdz. \tag{8}$$

Carrying out the integration in Eq. (8), we have:

$$\int_{z_{j-1/2}}^{z_{j+1/2}}(J_{i+1/2}-J_{i-1/2})\,dz + \int_{r_{i-1/2}}^{r_{i+1/2}}(Y_{j+1/2}-Y_{j-1/2})dr = \int_{r_{i-1/2}}^{r_{i+1/2}}\int_{z_{j-1/2}}^{z_{j+1/2}}(\Sigma_t\varphi - S)drdz. \tag{9}$$
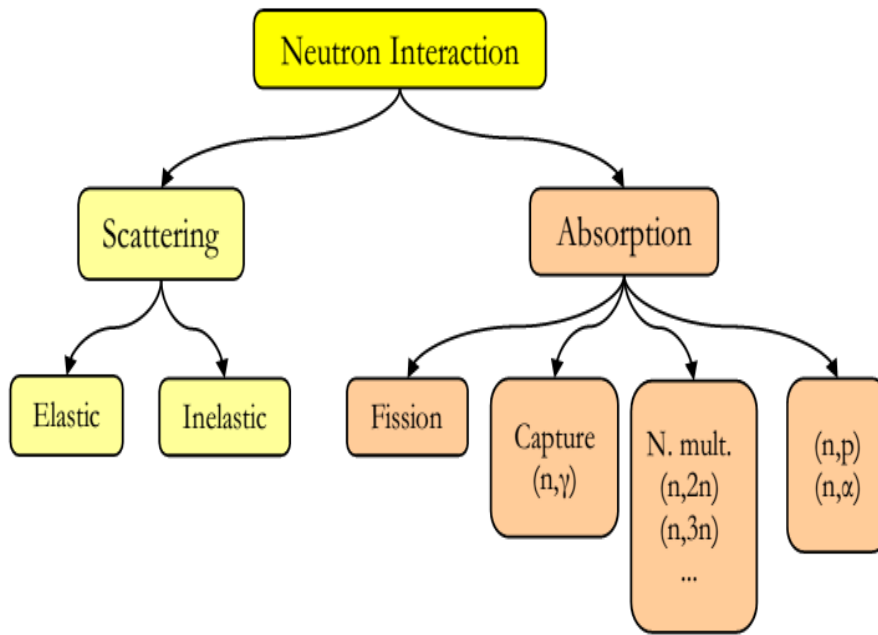
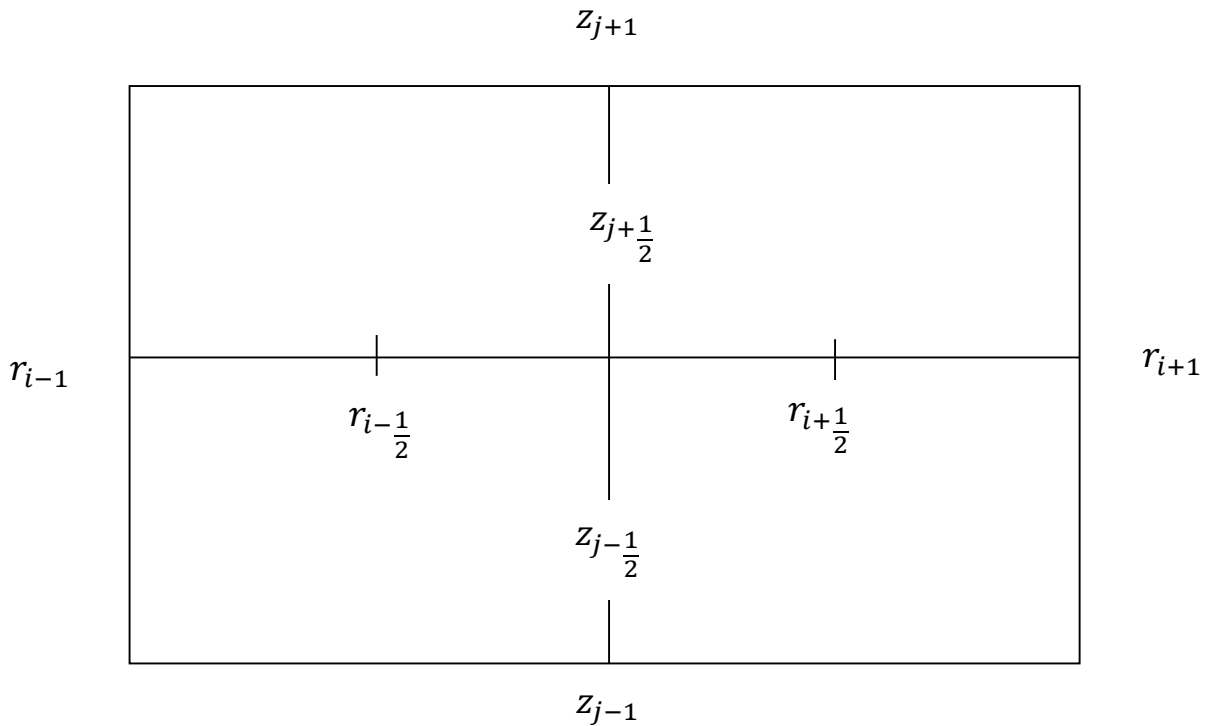Fig. 1. Types of neutron interaction with matter.

Fig. 2. Spatial mesh used for the finite difference approximation.

Each term in Eq. (9) can be written as Eqs. (10) and (11). Putting Eqs. (10), (11) and (12) into Eq. (9), we obtain Eq. (13). Integrating Eq. (5) over the interval $r_i < r < r_{i+1/2}$; $z_{j-1/2} < z < z_{j+1/2}$ eliminates J whilst an integration of Eq.(6) is performed over the limits $r_{i-1/2} < r < r_{i+1/2}$; $z_j < z < z_{j+1/2}$ eliminates Y. The simplified equation for the parameter J and Y can be written as Eq. (14), (15) and Eq. (16) and (17)

respectively. Putting Eqs. (14), (15), (16) and (17) into Eq. (13), we obtain Eq. (18). On further simplification of Eq. (18) and applying the boundary conditions, we obtain Eq. (19). The finite difference equation for the four-group diffusion equations in a cylindrical geometry can be obtained from Eq. (19). This is written as Group 1 (Eq. 20), Group 2 (Eq. 22), Group 3 (Eq. 23) and Group 4

(Eq. 24) respectively. The obtained four-group diffusion equations is the numerical solution for four-group diffusion equation in a cylindrical reactor core. Where,

$\Sigma_{s,g \to g+1}$ (Macroscopic scattering cross section from energy group g to $g+1$),

D_g (Neutron diffusion coefficient in energy group g),

$\Sigma_{a,g}$ (Macroscopic absorption cross section in energy group g) and

$v\Sigma_{f,g}$ is the source term giving the rate at which source neutrons appear in the group.

$$\int_{z_{j-1/2}}^{z_{j+1/2}} (J_{i+1/2} - J_{i-1/2}) \, dz = (J_{i+1/2} - J_{i-1/2})\Delta z_j \, , \tag{10}$$

$$\int_{r_{i-1/2}}^{r_{i+1/2}} (Y_{j+1/2} - Y_{j-1/2}) dr = (Y_{j+1/2} - Y_{j-1/2})r_i \Delta r_i \, , \tag{11}$$

$$\int_{r_{i-1/2}}^{r_{i+1/2}} \int_{z_{j-1/2}}^{z_{j+1/2}} (\Sigma_t \varphi - S) dr dz = (\sum_{t_{i,j}} \Delta r \Delta z)_{i,j} \varphi_{i,j} r_i - (S\Delta r\Delta z)_{i,j} r_i \, , \tag{12}$$

$$(J_{i+1/2} - J_{i-1/2})\Delta z_j + (Y_{j+1/2} - Y_{j-1/2})r_i \Delta r_i - (\sum_{t_{i,j}} \Delta r \Delta z)_{i,j} \varphi_{i,j} r_i = -(S\Delta r\Delta z)_{i,j} r_i \, . \tag{13}$$

$$J_{i+1/2,j} = \frac{D_{i+1/2,j} r_{i+1/2} \, \Delta z_j}{\Delta r_{i+1/2} \Delta z_{i+1/2,j}} [\varphi_{i+1,j} - \varphi_{i,j}] \, , \tag{14}$$

$$J_{i-1/2,j} = \frac{D_{i-\frac{1}{2},j} r_{i-\frac{1}{2}} \Delta z_j}{\Delta r_{i-\frac{1}{2}} \Delta z_{i-\frac{1}{2},j}} [\varphi_{i,j} - \varphi_{i-1,j}] \, , \tag{15}$$

$$Y_{i,j+1/2} = \frac{D_{i,j+1/2} \, \Delta r_i}{\Delta r_{i,j+1/2} \Delta z_{j+1/2}} [\varphi_{i,j+1} - \varphi_{i,j}] \, , \tag{16}$$

$$Y_{i,j-1/2} = \frac{D_{i,j-1/2} \, \Delta r_i}{\Delta r_{i,j-1/2} \Delta z_{j-1/2}} [\varphi_{i,j} - \varphi_{i,j-1}] \, , \tag{17}$$

$$\frac{D_{i+1/2,j} r_{i+1/2} \Delta z_j}{\Delta r_{i+1/2} \Delta z_{i+1/2,j}} (\varphi_{i+1,j} - \varphi_{i,j}) - \frac{D_{i-1/2,j} r_{i-1/2} \Delta z_j}{\Delta r_{i+1/2} \Delta z_{i+1/2,j}} (\varphi_{i,j} - \varphi_{i-1,j}) + \frac{D_{i,j+1/2} \, r_i \Delta r_i}{\Delta r_{i,j+1/2} \Delta z_{j+1/2}} (\varphi_{i,j+1} - \varphi_{i,j})$$
$$- \frac{D_{i,j-1/2} \, r_i \Delta r_i}{\Delta r_{i,j-1/2} \Delta z_{j-1/2}} (\varphi_{i,j} - \varphi_{i,j-1}) - r_{i,j} \sum_{t_{i,j}} \varphi_{i,j} \Delta r_i \Delta z_j = -r_{i,j} S_{i,j} \Delta r_i \Delta z_j \, . \tag{18}$$

$$\varphi_{i,j} = \frac{2Dr_i(\varphi_{i+1,j} + \varphi_{i-1,j} + \varphi_{i,j+1} + \varphi_{i,j-1}) + r_i[S_{i,j}]\Delta r\Delta z}{4Dr_i + r_i \Sigma_t} \, . \tag{19}$$

Group 1:
$$\varphi_{i,j}{}^1 = \frac{2D^1 r_i(\varphi_{i+1,j}{}^1 + \varphi_{i-1,j}{}^1 + \varphi_{i,j+1}{}^1 + \varphi_{i,j-1}{}^1) + r_i[S_{i,j}{}^1]}{4D^1 r_i + r_i \Sigma_{t_{i,j}}{}^1} \, , \tag{20}$$

$$\text{where} \qquad \Sigma_{t_{i,j}}{}^1 = \Sigma_{a1} \, , \tag{21}$$

and where the subscript represents the group number,

Group 2:
$$\varphi_{i,j}{}^2 = \frac{2D^2 r_i(\varphi_{i+1,j}{}^2 + \varphi_{i-1,j}{}^2 + \varphi_{i,j+1}{}^2 + \varphi_{i,j-1}{}^2) + \Sigma_{1 \to 2}\varphi_{i,j}{}^1}{4D^2 r_i + r_i \Sigma_{t_{i,j}}{}^2} \, , \tag{22}$$

$$\text{where} \qquad \Sigma_{t_{i,j}}{}^2 = \Sigma_{a2} + \Sigma_{1 \to 2} \, , \tag{23}$$

Group 3:

$$\varphi_{i,j}{}^3 = \frac{2D^3 r_i \left(\varphi_{i+1,j}{}^3 + \varphi_{i-1,j}{}^3 + \varphi_{i,j+1}{}^3 + \varphi_{i,j-1}{}^3\right) + \Sigma_{2\to3}\varphi_{i,j}{}^2}{4D^3 r_i + r_i \Sigma_{ti,j}{}^3} \qquad (24)$$

$$\text{where} \qquad \Sigma_{ti,j}{}^3 = \Sigma_{a3} + \Sigma_{1\to3} + \Sigma_{2\to3}, \qquad (25)$$

Group 4:

$$\varphi_{i,j}{}^4 = \frac{2D^3 r_i \left(\varphi_{i+1,j}{}^4 + \varphi_{i-1,j}{}^4 + \varphi_{i,j+1}{}^4 + \varphi_{i,j-1}{}^4\right) + \Sigma_{3\to4}\varphi_{i,j}{}^3}{4D^4 r_i + r_i \Sigma_{ti,j}{}^4}, \qquad (26)$$

$$\text{where} \quad \Sigma_{ti,j}{}^4 = \Sigma_{a4} + \Sigma_{1\to4} + \Sigma_{2\to4} + \Sigma_{3\to4}. \qquad (27)$$

Next, TUNTOB proceeds from the first group to the second, third and fourth group, iterating within each group until the criteria convergence is met. It evaluates the tolerance between the old and the new k_{eff} values. To calculate the new k_{eff}, the program integrates the old and new source terms over space and essentially averages them. With the updated source and k_{eff}, the iterations are performed again. The process continues until convergence is met. Next the program checks if the reactor is critical. If k_{eff} is very close to or equal to one (1), the system is critical. If the reactor is not critical, the program will again recommend an adjusted value for the core geometry, guessed multiplication factor (k) and flux.

3.2. Design of the Algorithm (TUNTOB)

The algorithm was designed using Matlab. Matlab was used because its algorithms can be developed in much shorter time than equivalent FORTRAN or C programs (Kiusalaas, 2005). The TUNTOB algorithm was developed for the criticality calculations of a homogenous cylindrical reactor core using four-group diffusion equations. The flow chart of the proposed algorithm is shown in Fig. 3.

4. RESULTS AND DISCUSSION

4.1. Iteration and Mesh Sizes Optimization

4.1.1. Iteration optimization

The calculations of the iteration optimization are shown in Table 1. A maximum of 1000 and a minimum of 600 iterations were performed. The 1000th iteration was performed for a 12 cm x 24 cm mesh size of the reactor core. The Table 1 shows the values of the effective multiplication factor of the same mesh size with the number of iterations (600-1000). It was observed that an increment in iteration leads to an increase in the effective multiplication factor obtained from 0.9983 to 0.9990 with a corresponding increase in the computation time. The maximum effective multiplication factor of (k_{eff} = 0.9990) was reached when the number of iterations were 1000 and above. Therefore, it was concluded that the optimal number of iterations required for this calculation is 1000.
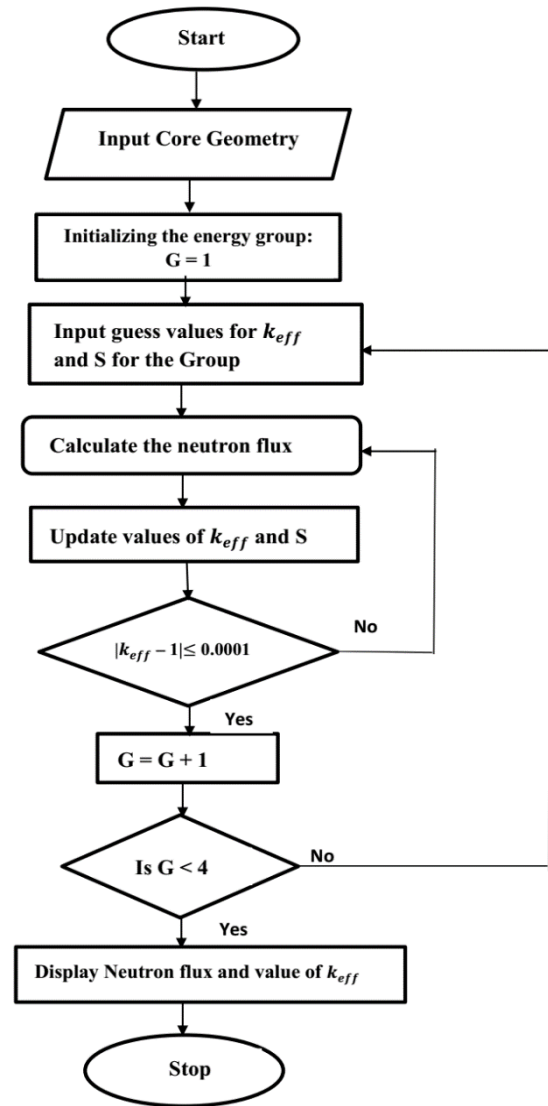

Fig. 3. Flow chart of the proposed algorithm (TUNTOB).

Table 1. Iterations optimization and its corresponding maximum effective multiplication factor (k_{eff}) with constant mesh size (4 cm x 4 cm).

Number of Iteration	Effective Multiplication Factor (k_{eff})	Computation Time (Min)
600	0.9983	2.818
700	0.9988	3.102
800	0.9989	3.592
900	0.9990	3.729
950	0.9990	3.845
1000	0.9990	4.282

4.1.2. Mesh size optimization

Having established the optimal number of iteration, the effects of the mesh size on the computation is examined in this section. The Table 2 reveals that the values of k_{eff} increases as the mesh sizes becomes smaller until an optimal mesh size of 1 x 1 cm^2 is reached and further decrease in mesh sizes gives no further improvement in the value of k_{eff}.

Table 2. Mesh size optimization and its corresponding maximum effective multiplication factor (k_{eff}) with constant 1000-iteration.

Mesh Size Area (cm^2)	Effective Multiplication Factor (k_{eff})	Computation Time (Min)
4 x 4	0.9990	4.282
2.4 x 2.4	0.9992	6.015
2 x 2	0.9996	6.751
1 x 1	0.9998	7.393
0.8 x 0.8	0.9998	8.491
0.5 x 0.5	0.9998	9.553

4.2. Neutron Flux Profile

The neutron flux profile was considered for both the axial and radial (3D) directions. This approach gave a better understanding of the behaviour of the neutron flux in the cylindrical reactor core. Comparing the results of the neutron flux distribution in the radial and axial directions obtained from TUNTOB with that of the neutron flux distribution of THESIS Code (Harman, 2001). It was observed that TUNTOB obtained better results than the THESIS Code, although, not all the THESIS source code parameters were accessible. In addition, we observed that the graphs of the THESIS Code follow the same trend with that obtained in this study.

4.2.1 Neutron flux distribution in 3-D representation

The color difference or variation in the neutron flux distribution for the 4 by 4 mesh from group 1 to group 4 confirms that the centre of the core has the greatest amount of heat (and the neutron flux has the highest value at the centre of the core) and the heat gradually reduces as the neutron flux moves away from the centre of the core until it gets to the surface of the core (from

color red, changes to color yellow and a light green color and then to color blue). The same trend occurs for other different mesh sizes for the four-group.

The neutron flux distributions in 3-D representation are shown in Fig. (4-11). The figures describe the behavior of the neutron flux for the four groups in both the radial and axial directions. The neutron flux profile showed that all the group behave in the same manner having maximum values at the center of the reactor core, (r = 0, z = H/2). The neutron flux for the first group (Group 1) has the highest maximum value, followed by the second (Group 2) and third group (Group 3) while the fourth group (Group 4) has the lowest. This trend is expected because fission neutrons are produced directly into the first three groups and the scattering of neutrons from these three groups serves as the source of neutrons in the fourth group. In Fig. (4-11), the 4 by 4 mesh showed that the trend of the flux in between the mesh points follows straight lines but when the number of mesh points is increased, the trend becomes a smooth curve as shown in Fig. (4-11) for a 1 by 1 mesh. It is expected that further increase in the number of mesh points will produce smoother curves with a corresponding increase in the computational time.
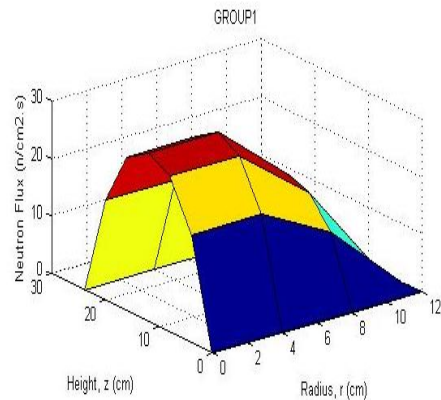

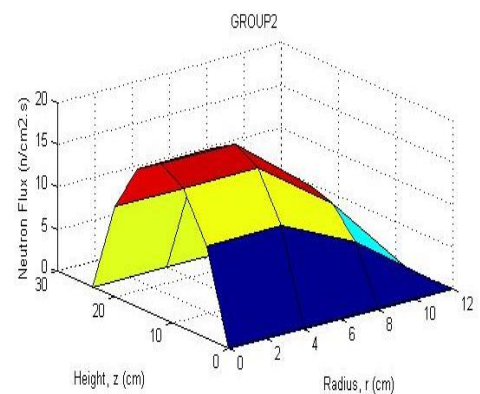Fig. 4. Neutron flux distribution in 3D for the first group of a 4 by 4 mesh.

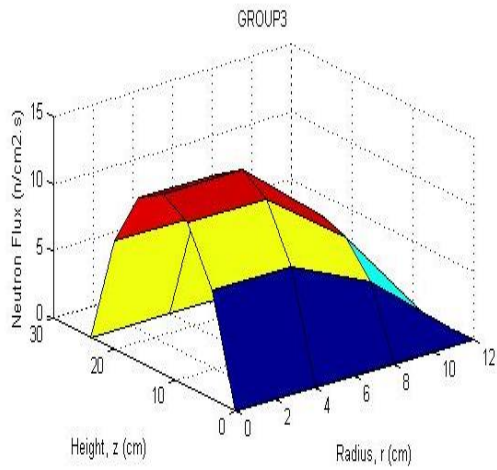Fig. 5. Neutron flux distribution in 3D for the second group of a 4 by 4 mesh.

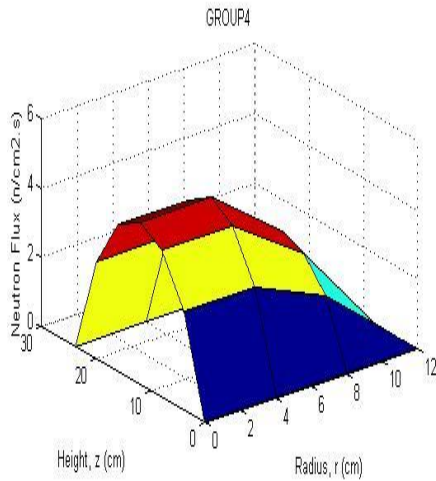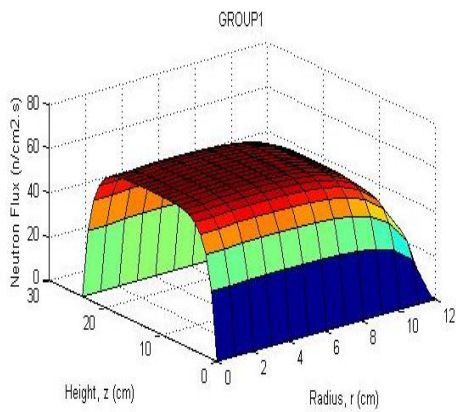Fig. 6. Neutron flux distribution in 3D for the third group of a 4 by 4 mesh.

Fig. 9. Neutron flux distribution in 3D for the second group of a 1 by 1 mesh.

Fig. 7. Neutron flux distribution in 3D for the fourth group of a 4 by 4 mesh.

Fig. 10. Neutron flux distribution in 3D for the third group of a 1 by 1 mesh.
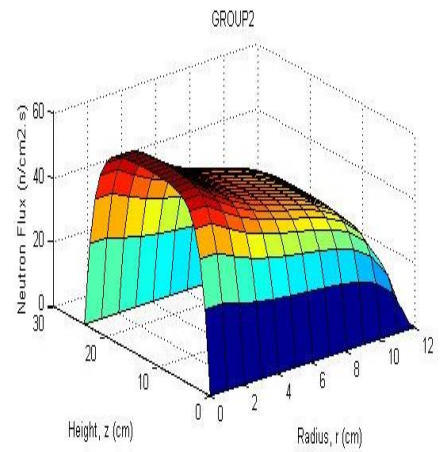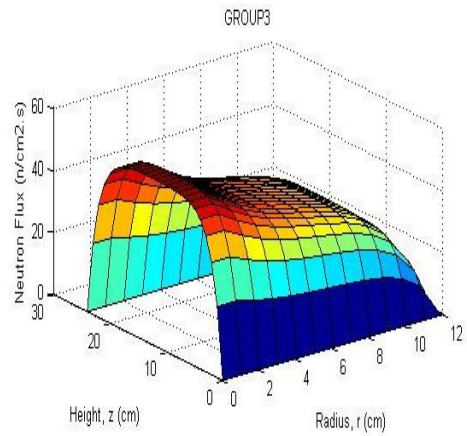

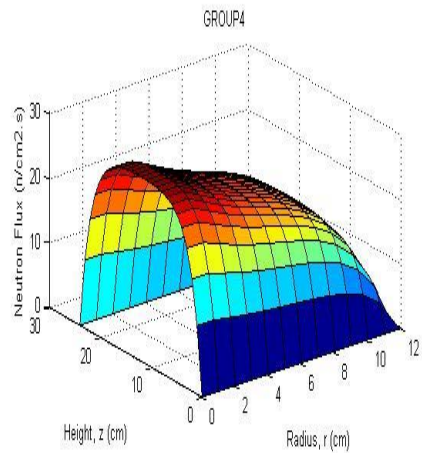Fig. 8. Neutron flux distribution in 3D for the first group of a 1 by 1 mesh.

Fig. 11. Neutron flux distribution in 3D for the fourth group of a 1 by 1 mesh.

In this work, we have derived four group diffusion equations for a cylindrical reactor core which gives a detailed description of neutron distribution in the core. We derived the discretized four group diffusion equations for a cylindrical reactor core because it gives an exact description of what takes place in a low water reactor (LWR). The results obtained for the criticality calculations were compared with criticality benchmarks and found to be very close. For instance, the k_{eff} calculated by the code is found to be 1.246728 while the benchmark value is 1.246368 (Ganapol, 2014).

CONCLUSION

This study provides the criticality calculation and neutron flux distribution in a homogenous cylindrical reactor core in two dimensions (r, z) using four energy groups. From the results these studies further confirm that the centre of the core of the reactor has the greatest heat which is synonymous to the different colour variations relating to decrease in the amount of heat as it moves away from the centre of the core. The calculations were carried out for a reactor in a steady state. The developed algorithm (TUNTOB), calculates values of k_{eff} and the neutron distribution as a function of the mesh sizes. It was found that the accuracy in the value of k_{eff} and the smoothness of the neutron distribution curves in 3-D representations, depends on the number of mesh points. It allows the user to modify the reactor dimensions and see the impacts on the neutron distribution and criticality within the reactor core.

ACKNOWLEDGEMENT

REFERENCE

Atomic Energy Control Board of Canada, *Fundamental of Power Reactors.* Canada: Atomic Energy Control Board of Canada (AECBC), pp. 1-3, 1993. Available [online]: http://www.thecanadianencyclopedia.ca/en/article/atomic-energy-control-board/

A. Arzhanov, *Analytical Models of Critical Reactor in Simple Geometries,* Royal Institute of Technology, Department of Physics. Stockholm, Sweden: KTH Engineering Sciences, pp. 1-33, 2010.

B. Ganapol, *Verification of the CENTRM Module for Adaptation of the SCALE Code to NGNP Prismatic and PBR Core Designs,* Univeristy of Arizona. Arizona: Reactor Concepts RD and D, 2014.

D. B. Ganapol, The Analytical Solution to the Multigroup Diffusion Equation in One - Dimensional Plane, Cylindrical and Spherical Geometries, *Joint International Tropical on Mathematics and Computation and Supercomputing in Nuclear Application,* 2007.

J. D. Burnham, Reactor Theory - The Steady State, *Nuclear Training Course,* 1967.

J. J. Duderstadt and J. L. Hamilton, *Nuclear Reactor Analysis.* Michigan: John Wiley and Sons, Inc, 672p, 1976.

J. T. Urbatsch, *Iterative Acceleration Methods for Monte Carlo and Deterministic Criticality.* California: Los Alamos National Laboratory, pp. 1-174, 1995. Available [online]: https://www.osti.gov/scitech/servlets/purl/212566

J. Kiusalaas, *Numerical Methods in Engineering with Matlab,* New York: Cambridge University Press, pp. 1-435, 2005.

M. A. Jayeola, M. K. Fasasi, A. A. Amosun, A. O. Salau, B. M. Ojo (2018), Numerical Computation of Fission-Product Poisoning Build-up and Burn-up Rate in a Finite Cylindrical Nuclear Reactor Core, *Bilge International Journal of Science and Technology Research,* Vol. 2(1), pp. 17-30.

M. S. Stacey, *Nuclear Reactor Physics.* Atlanta: Wiley-Vch Verlag Gmbh and Co. KGaA, Weinheim, 735p, 2007.

R. J. Larmash and J. A. Baratta, *Introduction to Nuclear Engineering (3ʳᵈ edition),* New Jersey, 420p, 2001.

T. Tanbay and O. Bilge, Numerical Solution of the Multigroup Neutron Diffusion Equation by the Meshless RBF Collocation Method, *Mathematical and Computational Applications,* Vol. 18, pp. 399-407, 2013.

W. H. Harman, Modelling Pressurized Water Reactor Kinetics, Ohio, Wright-Patterson Air Force Base, 2001.